A NOVEL COMPACT SIZE UWB BANDPASS FILTER WITH SHARP REJECTION SKIRT AND WIDE UPPER-STOPBAND BASED ON MULTIPLE-MODE-RESONATOR

Seyyed J. Borhani and Mohammad A. Honarvar[*]

Department of Electrical Engineering, Najafabad Branch, Islamic Azad University, Najafabad, Iran

Abstract—In this paper, a novel ultra-wideband (UWB) bandpass filter (BPF) based on multiple-mode resonator (MMR) is presented. The structure of the proposed MMR constructed by a modified triple-mode stepped-impedance resonator (SIR) loaded with a T-shape stub. This stub-loaded resonator can generate two more resonate modes and two transmission zeros (TZs) simultaneously. Five resonate modes of the proposed MMR are roughly allocated in the UWB pass band, as well as two TZs at the lower and upper cut-off frequencies of the passband, leading to sharp roll-off. Using aperture-backed interdigital-coupled lines for feeding, passband is realized, first harmonic resonate mode (sixth mode) suppressed by first TZ of the interdigital-coupled lines, and upper stopband extended. Resonant modes and TZs are discussed together. Finally, the proposed filter is fabricated and measured, and predicted results verified in measurement.

1. INTRODUCTION

Filters with compact size, sharp rejection skirt and good performance both in-band and out-of-band are highly required in UWB systems. On one hand, UWB filters must operate in very large transmission bandwidth, i.e., 3.1 to 10.6 GHz [1]. On the other hand, traditional synthesis design was systematically developed under the assumption of narrow passband. Therefore, the ultra-wide bandwidth specified by Federal Communications Commission (FCC) in 2002 creates a tremendous challenge in designing UWB BPF [2–15]. As a promising method, MMRs are widely utilized to design UWB bandpass

filters [2, 10]. In [2], MMR with stepped-impedance configuration was originally proposed to make use of its three first resonant modes to cover UWB passband. In [3–5], a quadruple-mode UWB BPF with wide upper stopband is proposed, but these filters suffer from poor selectivity. Later on, several quintuple-mode MMR-based UWB filters with varied configuration are proposed to improve selectivity, in-band and out-of-band performance [6–9]. In [6], upper stop-band is extended to 27 GHz, and [7] tries to fully cover UWB passband, but selectivity is still an issue in these filters. Selectivity and upper stop-band are improved in [8], but in-band insertion loss is 1.4 dB, and filter's size is large. [9] proposes UWB MMR-based which can have insertion loss less than 0.09 dB, but upper stop-band is narrow. In [10], a novel MMR structure is proposed for improving out-of-band rejection with two transmission zeros in upper stopband, but the drawback is roll-off at the lower and upper bands, and stopband is also narrow. In [11, 15], other methods and configurations are proposed to design UWB filter, but these filters also suffer from disadvantages in selectivity and size. Hence, it is still a challenge to improve size and selectivity of UWB BPFs while having good performance in- and out-of-band.

In this paper, a novel microstrip-line UWB BPF using modified MMR with compact size, sharp rejection skirt and wide upper stopband is presented. MMR is formed by a folded triple-mode stepped-impedance resonator (SIR) while uniform low-impedance line is replaced by a U-shaped low-impedance line is used to reduce overall size. A T-shape stub-loaded resonator is attached to the center of this modified SIR and can generate two more resonate modes and two TZs simultaneously. The first five resonant modes are roughly allocated in the UWB pass band, and two TZs at the lower and upper cut-off frequencies, i.e., 3.01/10.73 GHz. UWB passband is realized using a tight coupling between the MMR and input/output 50 Ω transmission lines. Aperture-backed interdigital-coupled lines are used for this purpose, and sixth resonant mode is suppressed as an effect by TZ of interdigital-coupled lines. Accordingly, sharp roll-off and compact size UWB BPF with good performance in- and out-of-band is obtained. Finally, the proposed filter is fabricated and measured to verify the predicted results. There is reasonable agreement between simulated and measured results.

2. CHARACTERISTICS OF THE PROPOSED MMR

Figure 1(a) shows the initial configuration of the proposed MMR-based UWB BPF. The proposed MMR is formed by a folded stepped-impedance resonator (FSIR) with the aim of placing two high-

impedance lines at the same side of the low-impedance line and to reduce the overall size, while uniform low-impedance line of FSIR is replaced by a U-shaped low-impedance line. FSIR is tuned to generate three resonate modes in the desired band. A T-shape stub is attached to the center of FSIR between two high-impedance lines. This stub can generate two more resonant modes and two TZs simultaneously. The lengths of high-impedance lines and U-shape low-impedance line are about $\lambda_g/4$ and $\lambda_g/2$, respectively (λ_g: guided-wavelength with respect to center frequency $f_0 = 6.85\,\text{GHz}$). In addition, interdigital-coupled lines are used for tight coupling between the MMR and $50\,\Omega$ feed-lines.

Since the structure is symmetric, even-odd method can be adopted to analyze it. Even and odd equivalent circuits of the proposed MMR are depicted in Figures 1(b) and (c), respectively.
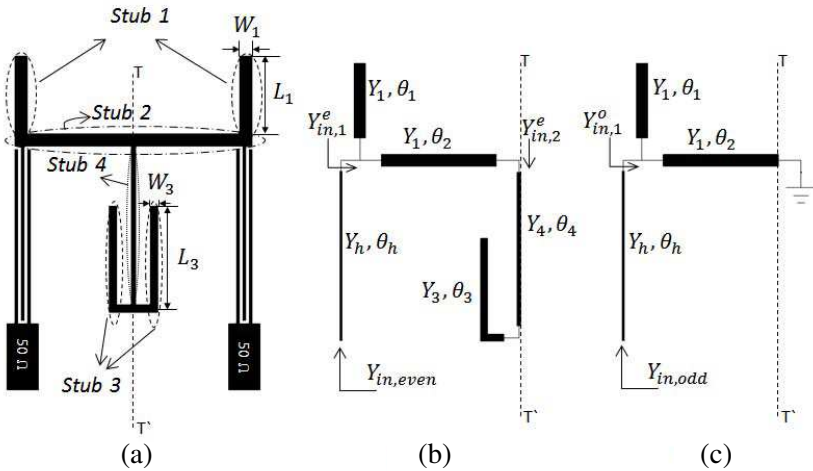

Figure 1. (a) Initial configuration of the proposed MMR-based UWB BPF. (b) Even-mode equivalent circuit of the proposed resonator. (c) Odd-mode equivalent circuit of the proposed resonator.

From the conditions $Y_{in,even} = 0$ and $Y_{in,odd} = 0$, the odd- and even-resonant frequencies can be extracted, respectively as following:

$$(Y_1 \tan\theta_1 + Y_h \tan\theta_h)(Y_1 Y_4 - Y_1 Y_3 \tan\theta_3 \tan\theta_4$$

$$-Y_3 Y_4 \tan\theta_2 \tan\theta_3 - Y_4^2 \tan\theta_2 \tan\theta_4) + Y_1 Y_3 Y_4 \tan\theta_3$$

$$+Y_1 Y_4^2 \tan\theta_4 + Y_1^2 \tan\theta_2(Y_4 - Y_3 \tan\theta_3 \tan\theta_4) = 0 \qquad (1)$$

$$Y_1 - Y_1 \tan\theta_1 \tan\theta_2 - Y_h \tan\theta_h \tan\theta_2 = 0 \qquad (2)$$

In addition, it can show:

$$S_{21} = \frac{y_{in,odd} - y_{in,even}}{(1 + y_{in,odd})(1 + y_{in,even})} \tag{3}$$

where $y_{in,odd} = Y_{in,odd}/Y_0$, $y_{in,even} = Y_{in,even}/Y_0$.

Obviously, when $Y_{in,even} = Y_{in,odd}$, TZs can be determined [10].

From Equations (1), (2) and Figures 1(b) and (c), it can be inferred that stub 1 and stub 2 control the position of both even and odd modes while stub 3 and stub 4 determine only the position of even modes, while the odd modes are fixed [8]. In the following, the effect of stub 1 and stub 3 on the resonant modes and TZs via EM simulator Agilent ADS Momentum are investigated. The resonator characteristics of the proposed MMR are realized under weak coupling.

Figure 2 shows the resonant modes and TZs of the proposed MMR with varied dimensions of stub 1, i.e., (L_1, W_1) while other dimensions kept fixed. As can be seen, five resonant modes and two TZs emerge in the range of UWB passband. As L_1 increases from 0 to 3.5 mm, f_{m4} tends to shift downwards significantly, which exerts a little effect on the other modes. Also, f_{z2} tends to shift downwards slightly more than f_{z1}. In addition, when W_1 varies from 0.3 to 0.5 mm, the fourth mode, f_{m4}, decreases significantly, while it has a little effect on the other modes and TZs [9]. Hence, the position of the fourth resonate mode can be flexibly controlled by the dimensions of stub 1.

As shown in Figure 3, when the length L_3 varies from 0 to 3.5 mm, while other dimensions kept fixed, f_{m1}, f_{m5}, f_{z1}, and f_{z2} shift downwards significantly. f_{m3} shifts slowly downwards, while the odd
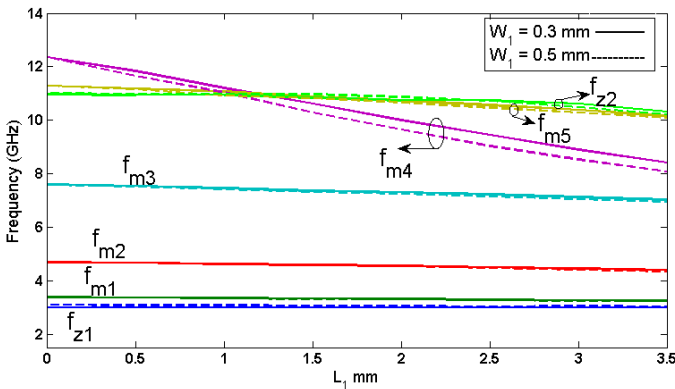

Figure 2. Effect of stub 1 (W_1, L_1) on the resonant modes and TZs while the other dimensions are kept fixed.

resonant modes (f_{m2}, f_{m4}) stay stationary and are not affected at all. As stub width W_3 is varied from 0.1 to 0.3 mm, the first and fifth mode frequencies, f_{m1} and f_{m5}, and two two TZs decrease dramatically while the other frequency modes are fixed. Therefore, the width of T-shaped stub can be used to adjust the resonant mode positions as an additional degree of freedom.
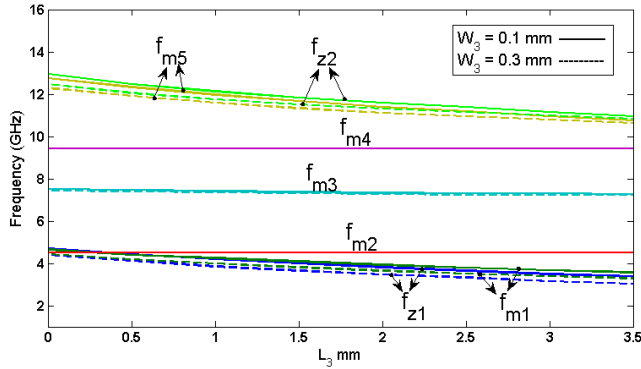

Figure 3. Effect of stub 3 (W_3, L_3) on the resonant modes and TZs while the other dimensions kept fixed.

3. SIMULATION AND MEASUREMENT OF THE PROPOSED UWB BPF

Based on the analysis in Section 2, five resonant modes of the proposed MMR, i.e., f_{m1} to f_{m5} and two TZs, i.e., f_{z1} and f_{z2}, can be utilized to make a compact UWB BPF with sharp skirt selectivity. Final configuration of the proposed UWB BPF is depicted in Figure 4, whereas slight differences between the initial layout and final configuration can be seen. First, the input/output of $50\,\Omega$ feed-lines are placed at two sides of the filter, also corners chamfered to reduce reflection. Second, for satisfactory cover UWB passband, the length of stub 4 needs to be long, hence this stub occupies less space, reducing overall size of the MMR, with a meander line replaced by a uniform line. In addition aperture in ground plan is created below the interdigital-coupled lines to increase coupling degree.

The final optimized dimensions of the proposed filter using EM simulator are: $L_1 = 2.45$, $W_1 = 0.3$, $L_2 = 7.5$, $W_2 = 0.4$, $L_{H1} = 1.1$, $L_{H2} = 0.75$, $L_{H3} = 1.6$, $L_3 = 3.75$, $W_3 = 0.25$, $L_p = 0.45$, $L_c = 7.6$, $L_g = 2.04$, $L_D = 4.75$, $W_D = 1.3$, $W_0 = 1$, $a = 2.1$, $b = 1$, $c = 0.25$,

Figure 4. Final configuration of the proposed UWB BPF.

$strip\_w = 0.1$, and $gap\_w = 0.1$ (all in millimeters). Relax line spacing, i.e., $gap\_w = 0.1$ mm, is obvious. The circuit size of the proposed MMR is 7.5 mm × 10.45 mm, or can be expressed as λ_g: $0.28\lambda_g \times 0.39\lambda_g$. The proposed UWB filter has compact size compared with previous UWB filters [3–16].

Simulated S_{21}-magnitudes of the proposed UWB BPF under weak coupling ($L_c = 1$ mm) and optimal coupling ($L_c = 7.6$ mm) are illustrated in Figure 5. First five resonate modes, i.e., $f_{m1} = 3.26$ GHz, $f_{m2} = 4.51$ GHz, $f_{m3} = 7.22$ GHz, $f_{m4} = 9.50$ GHz, and $f_{m5} = 10.48$ GHz, of the proposed MMR are located in UWB passband, as well as two TZs, i.e., $f_{z1} = 3.01$ GHz, and $f_{z2} = 10.73$, at lower and upper cut-off frequencies. In addition, first TZ of the aperture-backed interdigital-coupled lines, i.e., f_{zc}, suppresses f_{h1}, the first harmonic resonate mode. Moreover, simulated S_{21}-magnitudes of the modified triple-mode FSIR with and without T-shape stub under weak coupling for comparison are shown in Figure 6.

The proposed filter is fabricated on the Rogers_RO4003 substrate with relative dielectric constant: $\varepsilon_r = 3.38$, thickness: $h = 0.508$ mm and $\tan\delta = 0.0022$. Photographs of the fabricated UWB BPF are shown in Figure 7.

The performance of the filter is measured by Agilent 8722ES network analyzer. Figure 8 shows the simulated and measured results of the fabricated filter, and there is reasonable agreement between
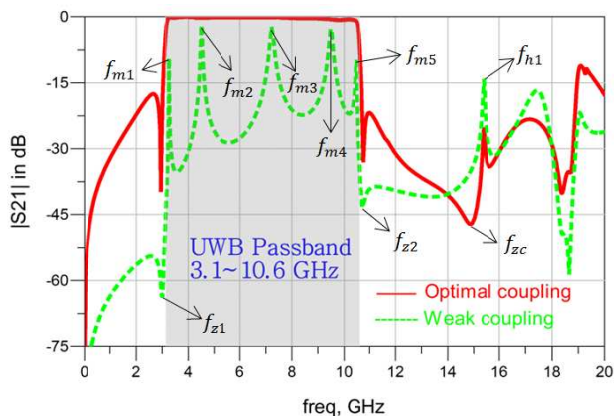
Figure 5. Simulated S_{21}-magnitude in dB of the proposed UWB BPF under weak and optimal coupling.
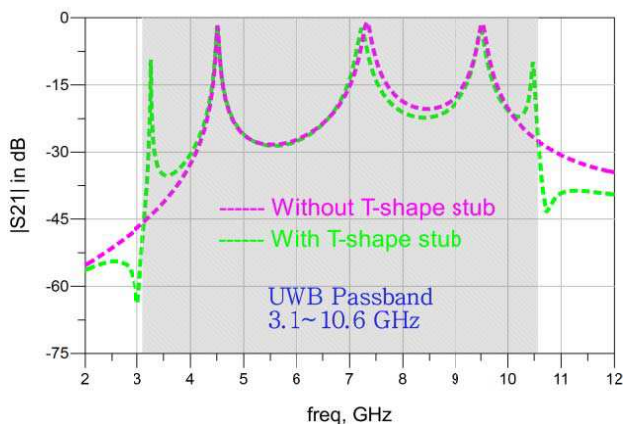

Figure 6. Simulated S_{21}-magnitude in dB of the modified triple-mode FSIR with and without T-shape stub under weak coupling.

simulated and measured results. Discrepancy between simulated and measured results and especially poor S_{11} may be due to unexpected tolerance in fabrication, material parameters and poor soldering craft.

3-dB bandwidth in simulation is from 3.15 to 10.58 GHz, which covers approximately 7.44 GHz, with center frequency: $f_0 = 6.86$ GHz and fractional bandwidth about: FBW = 108.34%. The filter has measured 3-dB bandwidth from 3.2 to 10.26 GHz and owes two TZs, $f_{z1} = 3.01$ GHz and $f_{z2} = 10.76$ GHz against its counterpart 3.01/10.73 GHz in simulation at the edge of the passband. At the
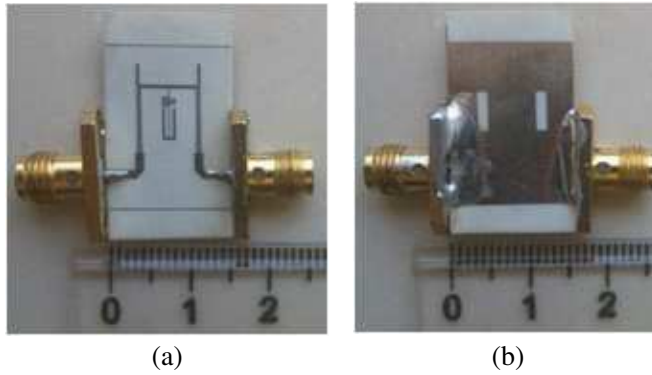
Figure 7. Photograph of the fabricated filter. (a) Top view. (b) Bottom view.
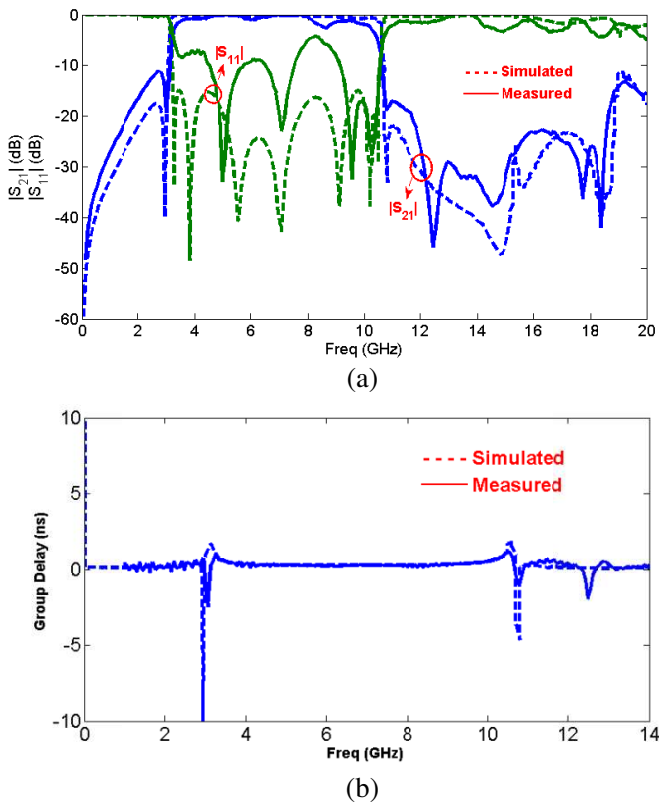

Figure 8. Simulated and measured results of the proposed filter (a) $|S_{21}|$ in dB and $|S_{21}|$ in dB. (b) Group delay.

center frequency, insertion loss in simulation and measurement is around 0.15 dB and better than 0.75 dB in the whole passband in simulation. Meanwhile, 1-dB insertion loss is in the range of 3.19–10.5 GHz in simulation. 30-dB bandwidth covers 7.78 GHz, so sharp factor can be calculated as fraction of 3-dB bandwidth to 30-dB bandwidth, i.e., 0.956, better than [2–16]. In simulation, return loss in whole bandwidth is better than 14.86 dB. Rejection level better than 20 dB in upper stopband is extended to around 18.5 GHz both in simulation and measurement, whereas the upper stopband of -10 dB level is extended to 20 GHz. In addition, group delay within the UWB passband in simulation and measurement is shown in Figure 8(b) with variation in simulation between 0.27–1.9 ns in comparison with measurement between 0.29–1.09 ns. Good linearity in most of the passband can be observed. Maximum peaks in lower and upper ends of the passband are caused by a trade-off between sharp rejection skirt and linearity in group delay [3]. Comparison between this work and other proposed filters is made in Table 1.

Table 1. Comparison with other proposed UWB filters.

Ref.	S.F. $\text{S.F.} = \frac{\Delta f\vert_{3\,\text{dB}}}{\Delta f\vert_{30\,\text{dB}}}$	FBW	f_c (GHz)	MMR Size $(\lambda_g \times \lambda_g)$
[5]	0.721	118% @ 2 dB	25.0	0.71×0.36
[8]	0.902	117% @ 3 dB	29.7	0.73×0.52
[9]	0.954	110.6% @ 3 dB	14.9	0.89×0.21
[10]	0.800	103.5% @ 3 dB	17.0	0.66×0.16
[13]	0.794	112.4 @ 3 dB	26.5	0.55×0.52
This Filter	0.956	108.34% @ 3 dB	18.5	0.28×0.39

f_c: the upper stopband frequency with 20 dB attenuation

4. CONCLUSION

A novel UWB BPF based on modified MMR and loaded with T-shape stub is presented and analyzed in this paper, and finally fabricated to verify predicted results. Dimensions of the proposed MMR are tuned, so that five resonant modes are located in UWB passband while two TZs at both sides of the passband leading to sharp roll-off. First TZ of the interdigital-coupled lines suppresses the first harmonic resonate mode, and wide upper stopband is realized. The filter has the advantage of compact size and sharp rejection skirt with

good performance in-band and out-of-band in UWB specification as confirmed in experimental. The proposed structure can be used in UWB systems either hand-held or indoor.

REFERENCES

1. FCC, "Revision of part 15 of the commission's rules regarding ultra-wideband transmission system," ET-Docket, 98–153, Washington, DC, Feb. 2002.

2. Zhu, L., S. Sun, and W. Menzel, "Ultra-wideband (UWB) bandpass filters using multiple-mode resonator," *IEEE Microw. Wireless Compon. Lett.*, Vol. 15, No. 11, 796–798, Nov. 2005.

3. Li, R. and L. Zhu, "Compact UWB bandpass filter using stub-loaded multiple-mode resonator," *IEEE Microw. Wireless Compon. Lett.*, Vol. 17, No. 1, 40–42, Jan. 2007.

4. Wong, S. W. and L. Zhu, "Quadruple-mode UWB bandpass filter with improved out-of-band rejection," *IEEE Microw. Wireless Compon. Lett.*, Vol. 19, No. 3, 152–154, Mar. 2009.

5. Honarvar, M. A. and R. A. Sadeghzadeh, "Design of coplanar waveguide ultrawideband bandpass filter using stub-loaded resonator with notched band," *Microwave Opt. Technol. Lett.*, Vol. 54, No. 9, 2056–2061, Sep. 2012.

6. Deng, H.-W., Y.-J. Zhao, X.-S. Zhang, L. Zhang, and S.-P. Gao, "Compact quintuple-mode UWB bandpass filter with good out-of-band rejection," *Progress In Electromagnetics Research Letters*, Vol. 14, 111–117, 2010.

7. Deng, H.-W., Y.-J. Zhao, L. Zhang, X.-S. Zhang, and W. Zhao, "Novel UWB BPF using quintuple-mode stub-loaded resonator," *Progress In Electromagnetics Research Letters*, Vol. 14, 181–187, 2010.

8. Wu, X. H., Q. X. Chu, X. K. Tian, and X. Ouyang, "Quintuple-mode UWB bandpass filter with sharp roll-off and super-wide upper stopband," *IEEE Microw. Wireless Compon. Lett.*, Vol. 21, No. 12, 661–663, Dec. 2011.

9. Shang, Z., X. Guo, B. Cao, B. Wei, X. Zhang, Y. Heng, G. Suo, and X. Song, "Design of a superconducting ultra-wideband (UWB) bandpass filter with sharp rejection skirts and miniaturized size," *IEEE Microw. Wireless Compon. Lett.*, Vol. 23, No. 2, 72–74, Feb. 2013.

10. Zhang, Z. and F. Xiao, "An UWB bandpass filter based on a novel type of multi-mode resonator," *IEEE Microw. Wireless Compon. Lett.*, Vol. 22, No. 10, 506–508, Oct. 2012.

11. Razalli, M. S., A. Ismail, and M. A. Mahdi, "Novel compact via-less ultra-wide band filter utilizing capacitive microstrip patch," *Progress In Electromagnetics Research*, Vol. 91, 213–227, 2009.

12. Huang, J.-Q. and Q.-X. Chu, "Compact UWB band-pass filter utilizing modified composite right/left-handed structure with cross coupling," *Progress In Electromagnetics Research*, Vol. 107, 179–186, 2010.

13. Tian, X.-K. and Q.-X. Chu, "A compact UWB bandpass filter with improved out-of-band performance using modified coupling structure," *Progress In Electromagnetics Research Letters*, Vol. 22, 191–197, 2011.

14. Nosrati, M. and M. Mirzaee, "Compact wideband microstrip bandpass filter using quasi-spiral loaded multiple-mode resonator," *IEEE Microw. Wireless Compon. Lett.*, Vol. 20, No. 11, 607–609, Nov. 2010.

15. Nosrati, M. and M. Daneshmand, "Compact microstrip ultra-wideband double/single notch-band band-pass filter based on wave's cancellation theory," *IET Microw. Antennas Propag.*, Vol. 6, No. 8, 862–868, Jun. 2012

16. Feng, W. J., W. Q. Che, Y. M. Chang, S. Y. Shi, and Q. Xue, "High selectivity fifth-order wideband bandpass filters with multiple transmission zeros based on transversal signal-interaction concepts," *IEEE Trans. on Microw. and Theory and Tech.*, Vol. 61, No. 1, 89–97, Jan. 2013.